

# RSGround-R1: Rethinking Remote Sensing Visual Grounding through Spatial Reasoning

Shiqi Huang<sup>1</sup> Shuting He<sup>2</sup> Bihan Wen<sup>1</sup>

## Abstract

Remote Sensing Visual Grounding (RSVG) aims to localize target objects in large-scale aerial imagery based on natural language descriptions. Owing to the vast spatial scale and high semantic ambiguity of remote sensing scenes, these descriptions often rely heavily on positional cues, posing unique challenges for Multimodal Large Language Models (MLLMs) in spatial reasoning. To leverage this unique feature, we propose a reasoning-guided, position-aware post-training framework, dubbed **RSGround-R1**, to progressively enhance spatial understanding. Specifically, we first introduce Chain-of-Thought Supervised Fine-Tuning (CoT-SFT) using synthetically generated RSVG reasoning data to establish explicit position awareness. Reinforcement Fine-Tuning (RFT) is then applied, augmented by our newly designed positional reward that provides continuous and distance-aware guidance toward accurate localization. Moreover, to mitigate incoherent localization behaviors across rollouts, we introduce a spatial consistency guided optimization scheme that dynamically adjusts policy updates based on their spatial coherence, ensuring stable and robust convergence. Extensive experiments on RSVG benchmarks demonstrate superior performance and generalization of our model.

## 1. Introduction

Remote Sensing Visual Grounding (RSVG) is a fundamental task in geospatial analysis that aims to accurately localize target objects within large-scale aerial imagery based on natural language descriptions (Sun et al., 2022; Zhan et al., 2023; Kuckreja et al., 2024; Li et al., 2024). This capability is essential for a wide range of applications, including mili-

<sup>1</sup>School of Electrical and Electronic Engineering, Nanyang Technological University <sup>2</sup>MoE Key Laboratory of Interdisciplinary Research of Computation and Economics, Shanghai University of Finance and Economics. Correspondence to: Bihan Wen <bihan.wen@ntu.edu.sg>.

Preprint. January 30, 2026.

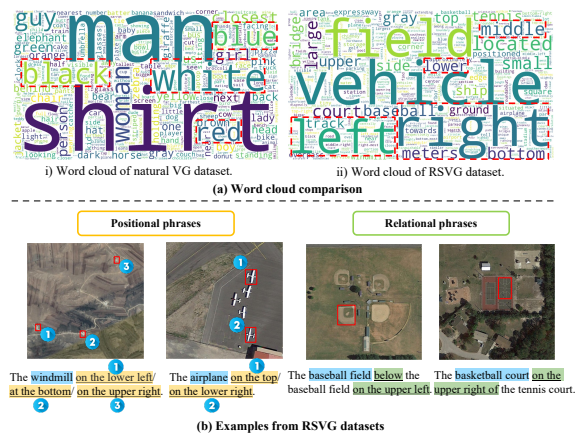


**Figure 1. (a)** Word cloud comparison between natural VG datasets RefCOCO+ (Yu et al., 2016), which relies exclusively on semantic attributes, and RSVG datasets (Zhan et al., 2023; Liu et al., 2024c; Li et al., 2024). Phrase size corresponds to its frequency. **(b)** Examples from DIOR-RSVG dataset (Zhan et al., 2023) with positional and relational phrases.

tary target identification, urban infrastructure mapping, and large-scale environmental monitoring (Zhan et al., 2023; Lobry et al., 2020; Ning et al., 2021; Lu et al., 2017). As remote sensing data from satellites and aerial platforms continue to grow exponentially, RSVG has become an indispensable tool for bridging human language queries with precise geospatial locations.

Despite recent progress in Vision-Language Models (VLMs) for Earth Observation (EO) tasks (Hu et al., 2025; Liu et al., 2024a; Wang et al., 2024b; Li et al., 2024), adapting these models to RSVG remains challenging. Remote sensing imagery differs fundamentally from natural images due to its vast spatial scale and high semantic ambiguity inherent in complex scenes (Huang et al., 2025a). As shown in Figure 1(a), natural visual grounding (VG) benchmarks such as RefCOCO+ (Yu et al., 2016) rely more on semantic attributes, such as color and texture, where target objects are typically salient and distinct. In contrast, linguistic expressions in RSVG depend predominantly on positional and relational cues. As illustrated in Figure 1(b), target objects in RSVG are often small, ambiguous, and non-unique (Zhan et al., 2023; Sun et al., 2022), requiring differentiation through positional descriptions such as “on the lower left” or “to the right of the tennis court”. This

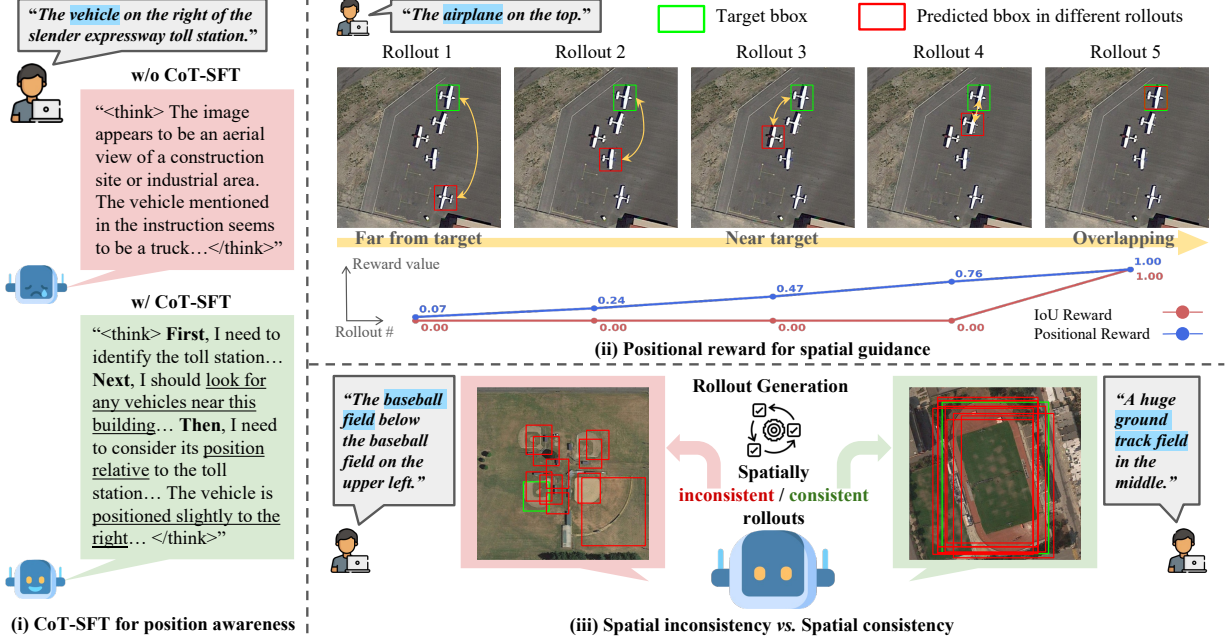


Figure 2. (i) **CoT-SFT for position awareness.** With CoT-SFT, the model can provide thinking process with clearer, position-aware spatial reasoning. (ii) **Positional reward for spatial guidance.** Positional reward increases as prediction approaches the target, whereas IoU reward remains zero. (iii) **Illustration of spatial inconsistency.** Samples representing spatially inconsistent/consistent rollouts.

paradigm shift makes spatial reasoning, rather than semantic recognition, the core challenge in RSVG, demanding fine-grained positional awareness across large and complex remote sensing scenes.

While Multimodal Large Language Models (MLLMs) demonstrate strong generalization abilities across diverse tasks, prior studies have shown that they often struggle with spatial reasoning (Fu et al., 2024; Majumdar et al., 2024; Zhang et al., 2024a; Wang et al., 2024a). Our preliminary experiment further reveal that MLLMs, such as Qwen2.5-VL (Bai et al., 2025a), fail to produce explicit spatial reasoning without structured spatial cues, as illustrated in Figure 2 (i), resulting in vague or semantically biased outputs for RSVG. To overcome this limitation, we introduce a specialized Supervised Fine-Tuning (SFT) stage termed **Chain-of-Thought SFT (CoT-SFT) for Position Awareness**. This stage leverages synthetically generated CoT data specifically designed to instill explicit and interpretable positional reasoning. Through this targeted preparation, the model is primed with a structured understanding of common spatial expressions in RSVG, establishing a solid foundation for subsequent reasoning enhancement.

After establishing positional reasoning awareness through CoT-SFT, we further enhance spatial precision via Reinforcement Fine-Tuning (RFT) with our spatially guided Group Relative Policy Optimization (GRPO) (Shao et al., 2024). Existing GRPO paradigms (Yang et al., 2025; Huang et al., 2025c; Shen et al., 2025) typically employ Intersection over Union (IoU) as a reward to supervise overall ground-

ing accuracy. However, as illustrated in Figure 2(ii), this feedback collapses to zero when the predicted region does not overlap with the ground truth, providing no informative gradient to distinguish near-miss predictions from entirely incorrect ones, e.g., those far from the target. Consequently, the model receives weak guidance for progressively refining its localization toward the target. To overcome this limitation and bridge the gap between high-level reasoning and fine-grained spatial precision in RSVG’s low-cue environment, we introduce a **Positional Reward for Spatial Guidance**. This continuous and distance-sensitive reward formulation provides smooth and informative feedback, effectively encouraging the model to iteratively adjust its predictions closer to the target region during RFT post-training.

Another key challenge we observe in RSVG during RFT training is the spatial inconsistency of rollouts generated from the same query, as demonstrated in Figure 2 (iii). This inconsistency arises from the characteristics of remote sensing imagery, which typically covers vast areas containing densely distributed and visually similar objects, making it difficult for the model to maintain coherent localization behavior across rollouts. As a result, the policy model often produces scattered predictions, weakening its spatial reasoning capability and overall grounding stability. To address this issue, we design a **Spatial Consistency Guided Optimization Scheme** that explicitly regulates the learning dynamics based on spatial coherence among rollouts. The mechanism quantifies the spatial dispersion of predictions within each query group and adaptively assigns higher weights to samples exhibiting greater inconsistency.

By directing the model’s focus toward these spatially diverse cases, the optimization promotes stable, contextually aligned grounding behavior.

In summary, this work presents the first principled study of spatial reasoning in MLLMs for RSVG, from the perspectives as follows:

- We introduce a cold-start CoT-SFT strategy that instills positional reasoning awareness, providing a structured initialization for RFT, leveraging our curated high-quality RSVG CoT dataset.
- We propose a positional reward that serves as a dense relaxation of IoU, enabling informative gradient signals even under zero-overlap conditions and facilitating progressive localization refinement.
- We develop a spatial consistency guided optimization scheme that modulates learning dynamics based on spatial coherence cues, enhancing stability and reliability during policy updates.
- Together, we propose **RSGround-R1**, which endows reasoning ability while achieving strong effectiveness and generalization across multiple RSVG benchmarks, despite using only a small fraction of the training data.

## 2. Related Work

### 2.1. Remote Sensing Visual Grounding

Remote sensing visual grounding (RSVG) aims to localize a target in aerial imagery from a natural-language description, requiring fine-grained spatial understanding. Early progress was established by Sun et al. (Sun et al., 2022), and extended by DIOR-RSVG (Zhan et al., 2023) with broaden categories and scene scale. Due to large spatial scale, complex semantics, and high inter-class similarity of aerial scenes (Hanyu et al., 2024; Yao et al., 2016; Huang et al., 2025a;b), the expressions in referring comprehensions rely largely on positional or relational phrases to disambiguate visually similar objects (Zhan et al., 2023; Yuan et al., 2023).

Despite progress, most existing RSVG approaches (Sun et al., 2022; Zhan et al., 2023) directly adapt general-purpose grounding or detection frameworks without explicitly modeling positional reasoning. These models often focus on category-level alignment rather than geometric understanding, leading to degraded performance under spatial ambiguity or scenes containing non-unique objects. As a result, there remains a clear need for methods capable of capturing explicit positional reasoning and geospatial consistency tailored to the unique characteristics of remote sensing data.

### 2.2. Remote Sensing VLMs

Advances in VLMs for natural images have driven the development of remote sensing foundation models for Earth

Observation (EO). Early works focus on image-level understanding using paired image–text data (Liu et al., 2024a; Wang et al., 2024b; Zhang et al., 2024b), while more recent MLLM-based models extend to region-level (Kuckreja et al., 2024; Pang et al., 2025; Muhtar et al., 2024; Li et al., 2025b; Luo et al., 2024) and pixel-level analysis (Shabbir et al., 2025; Ou et al., 2025; Li et al., 2025a). However, most existing remote sensing VLMs and MLLMs still rely heavily on vision–language contrastive pretraining (Radford et al., 2021) and supervised fine-tuning on EO tasks, which constrains their reasoning capability and generalization. Recent attempts to introduce RFT into remote sensing tasks (Koksal & Alatan, 2025; Muhtar et al., 2025; Yao et al., 2025; Jiang et al., 2025; Fiaz et al., 2025; Zhang et al., 2025; Liu et al., 2025) mostly are direct deployment of RL frameworks, without tailoring them to the characteristics of remote sensing data. Moreover, these approaches do not account for the distinctive spatial complexities inherent in geospatial imagery which is explicitly explored in our work.

Meanwhile, recent research reveals that most MLLMs still struggle with spatial reasoning (Fu et al., 2024; Majumdar et al., 2024; Zhang et al., 2024a; Wang et al., 2024a), prompting the development of general benchmarks that explicitly evaluate this ability (Liu et al., 2024d; 2023; Azzolini et al., 2025; Tian et al., 2025) and design of 3D-oriented spatial-aware models (Chen et al., 2024a; Cheng et al., 2024).

### 2.3. Reinforcement Fine-Tuning of VLMs

Reinforcement learning (RL) has become an effective post-training paradigm for enhancing multimodal reasoning in VLMs (Huang et al., 2025c; Guo et al., 2025; Shen et al., 2025). Methods such as DPO and PPO are widely used to align models with human or task-specific feedback (Rafailov et al., 2023; Schulman et al., 2017; Xie et al., 2024; Achiam et al., 2023; Zhai et al., 2024; Ma et al., 2024). More recently, GRPO introduces simple rule-based rewards to facilitate structured reasoning and has shown strong generalization on vision-language tasks (Shao et al., 2024; Guo et al., 2025; Yang et al., 2025; Huang et al., 2025c; Shen et al., 2025; Bai et al., 2025b), including referring expression comprehension and open-vocabulary detection (Shen et al., 2025). However, most existing RL-based reasoning frameworks remain concentrated on mathematical, coding, or general vision tasks, without specific consideration for remote-sensing scenarios.

## 3. Method

### 3.1. Overview

Our framework follows a two-stage pipeline. **CoT-SFT (Stage 1)**: we align the base model with high-quality, position-aware CoT data, establishing explicit positional

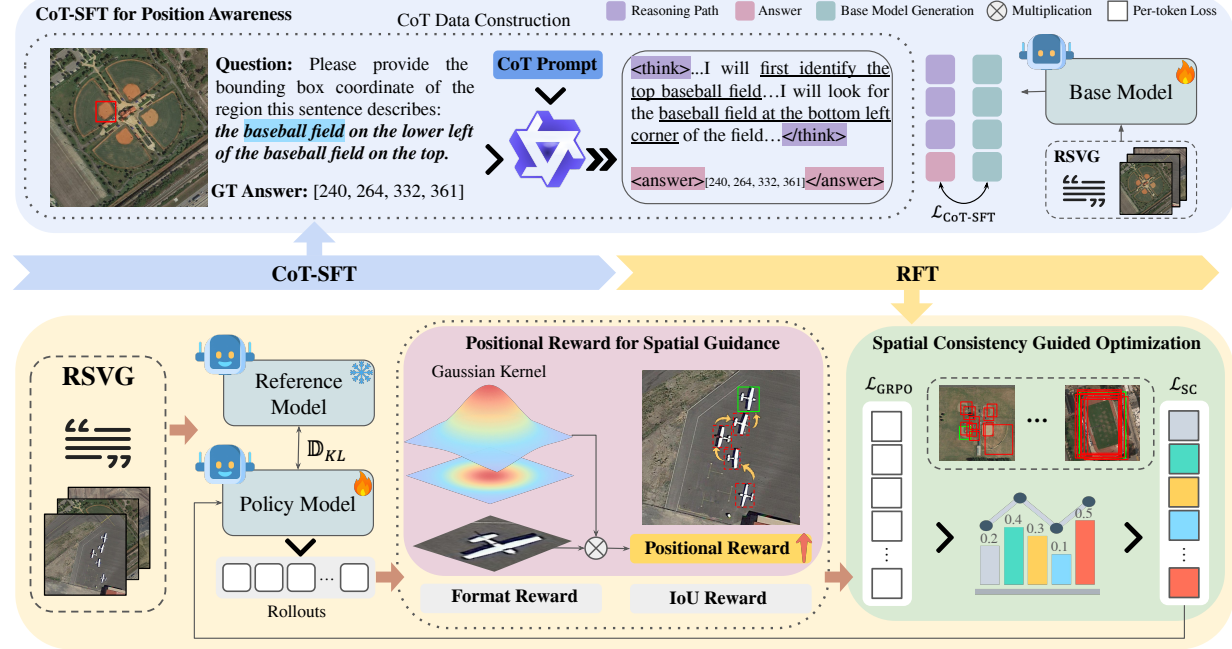


**Figure 3. Overview of RSGround-R1 pipeline.** Our framework has two consecutive stages. **CoT-SFT (Stage 1):** we curate high-quality, position-aware CoT data to finetune the base model and instill explicit positional understanding. **RFT (Stage 2):** after initializing the policy and reference model with the CoT-SFT finetuned based model, we further incentivize spatial reasoning using RFT by GRPO. Along with format and IoU rewards, we introduce a positional reward for progressive localization. To mitigate spatial inconsistent rollouts, we apply a spatial consistency guided optimization that reweights the per token GRPO loss  $\mathcal{L}_{\text{GRPO}}$  to yield  $\mathcal{L}_{\text{SC}}$ , promoting more stable and contextually aligned grounding behavior.

interpretability. **RFT (Stage 2):** we further incentivize spatial reasoning through RFT by augmenting GRPO with a positional reward and a spatial consistency guided optimization scheme. Together, these stages enable **RSGround-R1** to learn a deep, non-heuristic understanding of spatial relationships, yielding robust and reliable visual grounding capability for remote-sensing imagery.

### 3.2. CoT-SFT for Position Awareness

The first stage of our framework focuses on priming the model with explicit positional understanding before RFT. While general MLLMs such as Qwen2.5-VL (Bai et al., 2025a) or InternVL-2.5 (Chen et al., 2024b) possess strong multimodal alignment, they inherently lack spatial interpretability when handling remote sensing imagery. Their responses to positional queries are typically direct coordinate guesses without intermediate reasoning based on our preliminary inspection. To address this, we introduce the CoT-SFT stage which primes the model with positional understanding through explicit step-by-step reasoning traces.

**CoT Data Construction.** We first generate a CoT dataset focused on positional interpretation for RSVG. Given an annotated image–sentence pair  $(I, q, B_{gt})$ , where  $q$  is a referring expression and  $B_{gt}$  is its corresponding ground truth (GT) bounding box, we use the advanced MLLM Qwen2.5-

VL-72B (Bai et al., 2025a) to generate CoT reasoning process. Specifically, as illustrated in Figure 3, we provide the model with the question, GT bounding box coordinates, and a predefined CoT prompt, prompting it to generate reasoning processes in the format: “<think>thinking process here</think><answer>GT coordinates</answer>”.

Each generated sample is denoted as  $(I, q, r, B_{gt})$ , where  $r$  is the step-by-step reasoning path. To ensure data quality, we filter out responses that contain incomplete reasoning chains, inconsistent coordinate formats, or wrong bounding boxes. This process yields in a total of 30k synthetic CoT samples emphasizing spatial reasoning. More details are provided in the Appendices.

**CoT-SFT Cold Start Initialization.** We perform CoT-SFT on the base model Qwen2.5-VL-3B to guide the model in producing explicit and meaningful positional reasoning chains. The training objective is to maximize the conditional likelihood of producing the reasoning and answer sequence  $(r, B_{gt})$ , given the image-sentence pair  $(I, q)$ :

$$\mathcal{L}_{\text{CoT-SFT}} = -\mathbb{E}_{(I, q, r, B_{gt}) \sim \mathcal{D}} \left[ \sum_{t=1}^T \log \pi_{\theta}(y_t | I, q, y_{<t}) \right], \quad (1)$$

where  $\mathcal{D}$  is the CoT dataset,  $y$  is the concatenated sequence of  $r$  and  $B_{gt}$ , and  $\pi_{\theta}$  represents the model’s token distribu-

tion. The output model is then serves as the initialization of the policy and reference model in subsequent RFT stage.

This approach primes the model with a structured, step-by-step thinking process for RSVG queries, which gives the model a foundational understanding of the desired behavior before it is asked to explore and learn from reward signals in the more open-ended RL environment.

### 3.3. Positional Reward for Spatial Guidance

While the CoT-SFT stage equips the model with spatial reasoning priors for interpreting positions, it still lacks progressive spatial guidance during RFT. Standard GRPO implementations employ verifiable rewards such as format correctness or task accuracy (e.g., IoU between predicted and GT bounding boxes for VG task). However, IoU provides only a limited spatial signal: any predictions with zero overlap receive zero reward, offering no useful feedback for them to facilitate localization refinement. In the context of RSVG, where targets occupy small portions of extremely large images, this sparsity makes it difficult for the model to improve from completely wrong predictions. To provide continuous and spatially meaningful feedback, we design a positional reward that measures proximity between the predicted and target regions using a Gaussian proximity kernel. This kernel assigns higher values to predictions closer to the ground truth and lower values to distant ones, producing a smooth and progressive reward.

**Positional Reward Formulation.** Let  $B_p = [x_1^p, y_1^p, x_2^p, y_2^p]$  denotes the predicted bounding box and  $B_{gt}$  the ground truth. We define a Gaussian kernel  $\mathcal{K}(x, y)$  centered at the GT bounding box:

$$\mathcal{K}(x, y) = \exp\left(-\frac{(x - c_x^{gt})^2}{2\sigma_x^2} - \frac{(y - c_y^{gt})^2}{2\sigma_y^2}\right), \quad (2)$$

where  $(c_x^{gt}, c_y^{gt})$  is the ground-truth center,  $\sigma_x = \frac{\alpha W}{2}$ ,  $\sigma_y = \frac{\alpha H}{2}$ , with  $W$  and  $H$  being the box width and height. Here,  $\alpha$  controls the kernel deviations  $\sigma_x$  and  $\sigma_y$  based on  $W$  and  $H$ . We apply max-normalization to the kernel:

$$\hat{\mathcal{K}}(x, y) = \frac{\mathcal{K}(x, y)}{\max_{(u, v)} \mathcal{K}(u, v)}, \quad (3)$$

and compute the positional reward as the mean activation of this kernel within the predicted region:

$$R_{\text{pos}}(B_p, B_{gt}) = \frac{1}{|B_p|} \sum_{(x, y) \in \mathcal{P}(B_p)} \hat{\mathcal{K}}(x, y), \quad (4)$$

where  $\mathcal{P}(B_p)$  denotes the set of discrete pixel coordinates within the predicted bounding box. Intuitively, predictions that overlap or lie near to the ground-truth region receive higher scores, thereby encouraging far-off predictions to move toward the target by earning higher reward.

**Integration into GRPO** We combine the positional reward with the standard format reward and IoU reward (Shen et al., 2025; Yang et al., 2025) to form the overall verifiable signal:

$$R = R_{\text{format}} + R_{\text{IoU}} + \beta R_{\text{pos}}, \quad (5)$$

where  $\beta$  controls the contribution of positional proximity, balancing local spatial refinement with task correctness. During training, the reward is computed for each rollout and normalized across the group before computing the relative advantage in GRPO. This formulation allows the model to receive meaningful spatial gradients even when  $R_{\text{IoU}} = 0$ , effectively guiding the predicted boxes to progressively move closer to the target region through continuous positional feedback.

### 3.4. Spatial Consistency Guided Optimization

Due to the intrinsic characteristics of remote sensing imagery such as large spatial scales, visually similar or closely spaced objects within a scene, the rollouts generated frequently display noticeable spatial inconsistency for RSVG. This phenomenon reflects the model’s tendency to produce predictions that vary across different samples of the same query, leading to unstable localization behavior. To mitigate this issue, we introduce a spatial consistency guided optimization scheme that explicitly integrates spatial coherence into the policy update process.

To quantify the spatial consistency among multiple rollouts of the same query, we compute two statistics over their IoU rewards. Given a set of  $G$  rollouts, the mean and variance of IoU rewards are defined as:

$$m(\text{IoU}) = \frac{1}{G} \sum_{g=1}^G R_{\text{IoU}}^{(g)}, \quad (6)$$

$$\text{Var}(\text{IoU}) = \text{Var}(R_{\text{IoU}}^{(1)}, \dots, R_{\text{IoU}}^{(G)}). \quad (7)$$

These metrics jointly describe the spatial alignment of rollouts: higher  $m(\text{IoU})$  indicates accurate localization, whereas lower  $\text{Var}(\text{IoU})$  reflects coherent predictions across rollouts. We then derive an adaptive weighting factor that integrates these two signals into the optimization objective:

$$w = \exp(\lambda_m(1 - m(\text{IoU})) + \lambda_v \text{Var}(\text{IoU})), \quad (8)$$

which scales the per-token GRPO loss:

$$\mathcal{L}_{\text{SC}} = w \cdot \mathcal{L}_{\text{GRPO}}. \quad (9)$$

Here,  $\lambda_m$  and  $\lambda_v$  are coefficients controlling the contribution of mean accuracy and spatial variance, respectively. To ensure stability,  $w$  is clipped within  $[w_{\min}, w_{\max}]$ , where  $w_{\min} = 0.5$  and  $w_{\max} = 3.0$  in our implementation.

Table 1. Comparison with SOTA models. We evaluate both open-source general-purpose VLMs and RS-specific VLMs under zero-shot inference on RSVG datasets. Additionally, we report results of finetuned RS-VLMs to provide a comprehensive in-domain evaluation. Methods marked with \* indicates SFT for 1 epoch, while † denotes GRPO-based RFT training for only 0.4 epoch using 40% of the training data. **Bold** and underline represent the best and second best results. We report the average results over three independent runs.

Method	Params	DIOR-RSVG			VRSBench-VG			RRSIS-D		
		@0.5	@0.7	mIoU	@0.5	@0.7	mIoU	@0.5	@0.7	mIoU
<i>General Vision-Language Models</i>										
MiniGPT-v2 (Chen et al., 2023)	7B	30.25	11.46	30.08	35.84	16.82	34.72	37.26	15.88	38.65
LLaVA-1.5 (Liu et al., 2024b)	7B	16.07	4.15	23.15	15.29	3.43	23.93	16.09	4.08	24.60
Qwen2.5-VL-3B (Bai et al., 2025a)	3B	37.50	26.25	37.31	38.25	19.65	37.03	38.75	26.05	39.22
Qwen2.5-VL-7B (Bai et al., 2025a)	7B	39.25	25.20	38.66	43.60	22.90	41.13	41.95	26.30	41.08
<i>Remote Sensing Vision-Language Models</i>										
GeoChat (Kuckreja et al., 2024)	7B	25.95	4.53	29.87	14.19	2.29	23.66	24.36	3.94	30.30
VHM (Pang et al., 2025)	7B	52.15	25.63	46.01	23.48	4.43	28.92	61.39	42.92	53.10
SkySenseGPT (Luo et al., 2024)	7B	22.86	5.52	27.76	11.00	2.22	21.25	24.81	6.48	29.63
LHRS-Bot (Muhtar et al., 2024)	7B	12.49	3.02	17.91	1.40	0.20	8.23	16.81	3.43	21.59
LHRS-Bot-Nova (Li et al., 2025b)	8B	32.87	12.37	31.61	18.30	4.30	25.98	39.41	16.86	36.39
<i>w/ training</i>										
<i>Remote Sensing Vision-Language Models</i>										
GeoChat w/ SFT*	7B	46.48	13.30	43.05	59.27	32.61	52.03	50.82	20.77	45.33
VHM w/ SFT*	7B	61.67	45.73	54.85	56.48	30.07	49.71	62.31	44.67	54.19
Qwen2.5-VL-3B w/ SFT*	3B	62.60	47.60	55.71	61.85	36.55	53.22	62.60	47.40	55.95
Qwen2.5-VL-3B w/ GRPO†	3B	66.65	56.15	60.18	59.25	36.00	51.23	58.50	44.20	53.60
<b>RSGround-R1†</b>	3B	<b>71.81</b>	<b>58.71</b>	<b>63.38</b>	<b>63.72</b>	<b>38.32</b>	<b>54.68</b>	<b>65.73</b>	<b>50.04</b>	<b>58.35</b>

By incorporating this adaptive weighting based on spatial coherence, we derive the resulting spatial consistency loss  $\mathcal{L}_{SC}$ . This optimization dynamically emphasizes predictions with higher dispersion, guiding the policy toward stable and spatially consistent grounding behavior.

## 4. Experiment

### 4.1. Datasets and Metrics

**Training Dataset.** We train the model on multiple remote sensing visual grounding datasets, including widely used benchmarks DIOR-RSVG (Zhan et al., 2023), as well as datasets with grounding annotations such as VRSBench (Li et al., 2024) and RRSIS-D (Liu et al., 2024c). We denote the visual grounding subset of VRSBench as VRSBench-VG. Together, these datasets represent a diverse cover diverse object categories, instance densities, and scene complexities, and include a wide range of referring expressions, such as positional, directional, and relational descriptions.

**Evaluation Dataset.** We validate our method from two complementary perspectives: in-domain evaluation and out-of-domain generalization. In-domain evaluation is conducted on the official test splits of DIOR-RSVG, VRSBench-VG, and RRSIS-D. To assess out-of-domain generalization, we further employ the visual-grounding-annotated FAST-T and SOTA-T datasets (Wang et al., 2023) from GeoPixInstruct (Ou et al., 2025), ensuring no overlap with the training

data to rigorously assess cross-domain generalization. For models fine-tuned on VRSBench-VG, SOTA-T is excluded since it is derived from DOTA (Ding et al., 2021), which is included in VRSBench-VG.

**Evaluation Metrics.** We adopt the conventional evaluation protocol used in visual grounding. Specifically, we report Accuracy (Acc), where a prediction is regarded as correct if its Intersection over Union (IoU) with the ground-truth bounding box exceeds a predefined threshold (0.5 for Acc@0.5 and 0.7 for Acc@0.7). We also report the mean IoU (mIoU) to provide a more detailed assessment of localization precision and overall grounding performance.

### 4.2. Model and Implementation Details

We employ Qwen2.5-VL-3B-Instruct (Bai et al., 2025a) as the base model. Our implementation is built upon VLM-R1 (Shen et al., 2025), following its default hyperparameter settings unless otherwise specified. For GRPO-based RFT, we train the model for 0.4 epoch using only 40% of each training dataset, which substantially improves data-efficiency while still achieving superior performance. For experiments with SFT, we finetune each method for 1 epoch using the full training set of each RSVG dataset. In our experiments, the positional reward is configured with  $\beta = 0.1$  and  $\alpha = 2.5$ . For spatial consistency guided optimization, we set  $\lambda_m = 1.2$  and  $\lambda_v = 1$ .

Table 2. Out-of-domain generalization. We assess the models’ generalization capability on the FAST-T and SOTA-T datasets, ensuring that no data overlap exists between the training and testing sets. **Bold** and underline represent the best and second best results.

Method	DIOR-RSVG						VRSBench-VG						RRSIS-D					
	FAST-T			SOTA-T			FAST-T			FAST-T			SOTA-T					
	@0.5	@0.7	mIoU	@0.5	@0.7	mIoU												
GeoChat w/ SFT*	20.81	4.65	25.77	15.87	3.99	20.66	26.93	8.17	28.21	11.73	2.21	18.56	9.11	2.60	14.14			
VHM w/ SFT*	16.69	4.59	21.88	14.40	4.56	18.43	29.08	11.71	28.38	9.35	2.09	15.75	9.11	2.60	13.24			
Qwen2.5-VL-3B w/ SFT*	27.78	10.92	29.80	27.58	9.11	27.78	43.70	21.10	37.02	27.55	11.11	29.65	27.99	9.36	27.63			
Qwen2.5-VL-3B w/ GRPO <sup>†</sup>	<u>36.55</u>	<u>18.44</u>	<u>35.66</u>	<u>34.58</u>	<u>17.58</u>	<u>31.27</u>	<u>47.49</u>	<u>27.36</u>	<u>39.63</u>	<u>33.49</u>	<b>17.19</b>	<b>32.92</b>	<u>30.59</u>	<u>15.20</u>	<u>28.20</u>			
<b>RSGround-R1<sup>†</sup></b>	<b>38.59</b>	<b>19.21</b>	<b>35.96</b>	<b>38.00</b>	<b>19.69</b>	<b>33.25</b>	<b>49.71</b>	<b>28.05</b>	<b>39.93</b>	<b>35.49</b>	<u>16.7</u>	<u>32.45</u>	<u>32.79</u>	<u>15.54</u>	<b>29.50</b>			

Table 3. Component Analysis: CoT-SFT, positional reward  $R_{\text{pos}}$  and spatial consistency guided optimization  $\mathcal{L}_{\text{SC}}$ .

Components			DIOR-RSVG		
CoT-SFT	$R_{\text{pos}}$	$\mathcal{L}_{\text{SC}}$	@0.5	@0.7	mIoU
✗	✗	✗	66.65	56.15	60.18
✓	✗	✗	68.45	56.70	60.43
✗	✓	✗	68.10	56.85	61.12
✗	✗	✓	69.95	57.65	62.44
✓	✓	✓	<b>71.81</b>	<b>58.71</b>	<b>63.38</b>

### 4.3. Main Results

**Comparison with SOTA models** Table 1 compares our method with both general-purpose and remote-sensing-specific VLMs. Among general VLMs, Qwen2.5-VL (Bai et al., 2025a) consistently outperforms MiniGPT-v2 (Chen et al., 2023) and LLaVA-1.5 (Liu et al., 2024b), and even outperforms several RS-specific models such as GeoChat (Kuckreja et al., 2024), SkySenseGPT (Luo et al., 2024), LHRs-Bot (Muhtar et al., 2024) and LHRs-Bot-Nova (Li et al., 2025b), highlighting the limitations of existing RS VLMs in addressing remote-sensing visual grounding. While RS-specific models improve after fine-tuning and GRPO-based RFT shows competitive performance, our method consistently achieves the best results. Notably, **RSGround-R1** surpasses direct GRPO by over 5% in Acc@0.5 using only 0.4 epoch (40% data), demonstrating superior learning effectiveness and generalization.

**Out-of-domain Generalization** Table 2 evaluates the out-of-domain generalization on the FAST-T and SOTA-T benchmarks, which introduce significant regional and sensor shifts. SFT-based methods perform worse than GRPO-based counterparts, highlighting the difficulty of transferring grounding ability through supervised tuning alone. **RSGround-R1** consistently outperforms the GRPO baseline, especially on SOTA-T, demonstrating strong robustness and transferable spatial priors under substantial domain shifts.

### 4.4. Ablation Study

**Component Analysis** Table 3 summarizes the contribution of each component on the DIOR-RSVG dataset. The

Table 4. Positional reward for spatial guidance: comparisons with alternative distance-aware reward functions.

Reward Functions	DIOR-RSVG		
	@0.5	@0.7	mIoU
<b>IoU</b> [Baseline]	66.65	56.15	60.18
<b>+GIoU</b>	65.10	54.05	58.87
<b>+DIoU</b>	63.60	53.45	57.43
<b>+Center distance</b>	67.40	56.33	60.81
<b>+<math>R_{\text{pos}}</math> [Ours]</b>	<b>68.10</b>	<b>56.85</b>	<b>61.12</b>

Table 5. Spatial consistency guided optimization: effect of m(IoU) and Var(IoU) in the spatial consistency weighting.

DIOR-RSVG		
m(IoU)	Var(IoU)	@0.5
✗	✗	66.65
✓	✗	68.68
✗	✓	67.80
✓	✓	<b>69.95</b>
		<b>57.65</b>
		<b>62.44</b>

first row without any components denotes the pure GRPO-based RFT baseline. As seen from the second row, incorporating CoT-SFT yields about a 3% improvement in Acc@0.5, validating the importance of establishing a positional reasoning foundation. The additional gain achieved by introducing the positional reward  $R_{\text{pos}}$  also demonstrates the effectiveness in guiding the model toward spatially aligned predictions. Integrating the spatial consistency loss  $\mathcal{L}_{\text{SC}}$  provides 3.3% improvement in Acc@0.5 by stabilizing predictions across rollouts. When all three components are combined, the model achieves the best overall performance, confirming their complementary contributions to robust spatial reasoning and grounding precision.

**Positional Reward** Table 4 compares our positional reward  $R_{\text{pos}}$  with other distance-aware functions such as GIoU, DIoU and center distance as rewards. Although they provide non-zero gradients under non-overlapping conditions, applying them as reward functions brings limited or even negative effects. Unlike box-level or distance penalties that can induce noisy and high-variance signals in policy learning,  $R_{\text{pos}}$  offers smooth, scale-adaptive proximity feedback, leading to more stable and informative optimization.

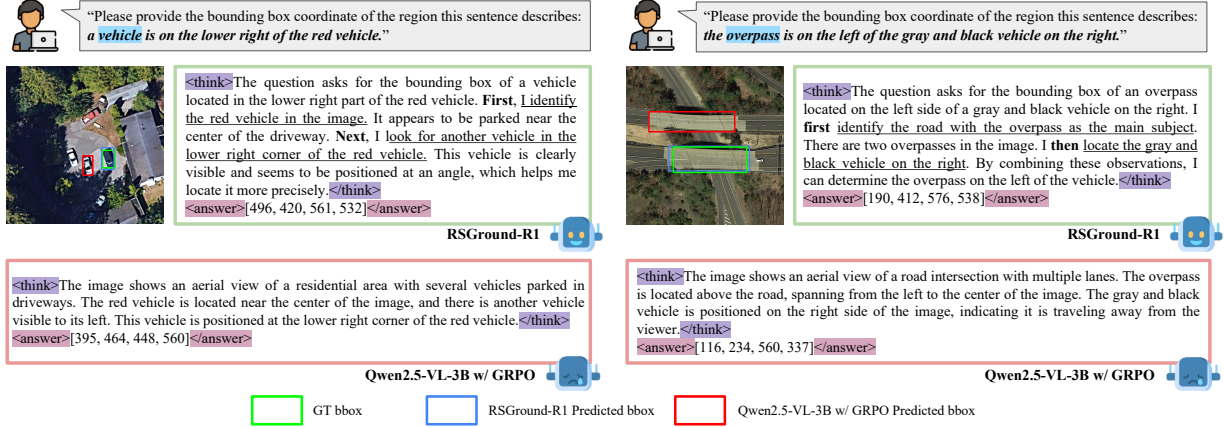


Figure 4. Qualitative comparison. **RSGround-R1** produces more plausible reasoning trajectories and more accurate bounding box predictions compared to the baseline Qwen2.5-VL-3B w/ GRPO. More visualizations can be found in the Appendices.

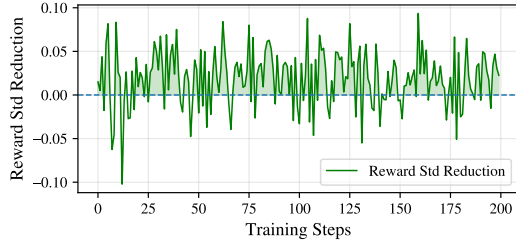


Figure 5. Spatial consistency guided optimization: reward std reduction vs. baseline on DIOR-RSVG dataset.

**Spatial Consistency** Table 5 analyzes the effect of incorporating mean and variance terms in the spatial consistency weighting. Using only the mean IoU reward emphasizes overall localization quality, leading to a clear improvement of 2% in Acc@0.5. Incorporating only the variance term enhances stability by penalizing inconsistent rollouts, resulting in a 1% gain. Combining both m(IoU) and Var(IoU) achieves the best performance, demonstrating that joint consideration enables more balanced policy updates and improves grounding precision and robustness.

Figure 5 visualizes the reduction in reward standard deviation after applying  $\mathcal{L}_{sc}$ . The consistently lower variance across training steps suggests that spatial consistency guided optimization effectively stabilizes rollout behavior, leading to smoother and more reliable policy optimization.

#### 4.5. Qualitative Comparison

The comparison highlights the distinct reasoning and localization behaviors between RSGround-R1 and Qwen2.5-VL-3B w/ GRPO. Qwen2.5-VL-3B w/ GRPO produces a concise yet surface-level response, directly describing visible objects without explicitly decomposing the spatial relationship. Its bounding box prediction aligns with the target object class but shows a positional offset. In contrast, **RSGround-R1** demonstrates a more structured and step-wise reasoning process. This progressive reasoning yields more accurate localization and exemplifies the benefits of Chain-of-Thought SFT combined with spatially guided RFT.

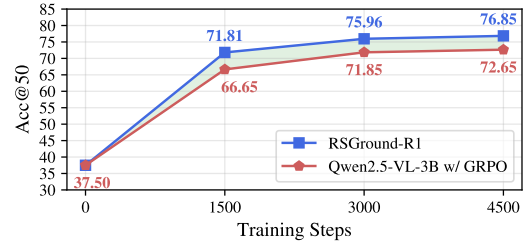


Figure 6. Performance under extended training process beyond the default 0.4-epoch (1500 steps) setting on DIOR-RSVG dataset. More comparisons are provided in the Appendices.

Overall, **RSGround-R1** exhibits superior interpretability and spatial awareness, reasoning through multi-step relationships rather than relying on direct visual matching alone.

#### 4.6. Performance under Extended Training

Figure 6 illustrates the sustained benefits of our design by extending training beyond 0.4 epoch (1500 steps) on the DIOR-RSVG dataset and evaluating performance at 1500-step intervals. As training progresses, our method continues to yield steady gains and consistently outperforms the GRPO fine-tuning baseline. These results show that positional reasoning and spatial consistency optimization not only accelerate early-stage learning but also deliver continuous improvements during prolonged training, demonstrating the robustness and scalability of our approach.

## 5. Conclusion

In this work, we presented **RSGround-R1**, a reasoning-guided, position-aware post-training framework for remote sensing visual grounding that addresses the task’s inherent spatial reasoning challenges. By combining CoT-SFT using our curated CoT data with reinforcement learning enhanced by positional reward and spatial consistency optimization, our approach improves localization accuracy, training stability, and generalization across diverse benchmarks. The interpretability and robustness of our model present a promising direction for advancing geospatial understanding.

## Impact Statement

While remote sensing visual grounding has beneficial applications in urban planning, disaster assessment, and environmental monitoring, it may also be subject to dual-use risks, including misuse for surveillance or military purposes. We emphasize that the proposed model is intended for research and large-scale scene understanding, rather than individual-level monitoring. Beyond these considerations, we do not identify additional impacts that require specific discussion.

## References

Achiam, J., Adler, S., Agarwal, S., Ahmad, L., Akkaya, I., Aleman, F. L., Almeida, D., Altenschmidt, J., Altman, S., Anadkat, S., et al. Gpt-4 technical report. *arXiv preprint arXiv:2303.08774*, 2023.

Azzolini, A., Bai, J., Brandon, H., Cao, J., Chattopadhyay, P., Chen, H., Chu, J., Cui, Y., Diamond, J., Ding, Y., et al. Cosmos-reason1: From physical common sense to embodied reasoning. *arXiv preprint arXiv:2503.15558*, 2025.

Bai, S., Chen, K., Liu, X., Wang, J., Ge, W., Song, S., Dang, K., Wang, P., Wang, S., Tang, J., et al. Qwen2.5-vl technical report. *arXiv preprint arXiv:2502.13923*, 2025a.

Bai, S., Li, M., Liu, Y., Tang, J., Zhang, H., Sun, L., Chu, X., and Tang, Y. Univg-r1: Reasoning guided universal visual grounding with reinforcement learning. *arXiv preprint arXiv:2505.14231*, 2025b.

Chen, B., Xu, Z., Kirmani, S., Ichter, B., Sadigh, D., Guibas, L., and Xia, F. Spatialvlm: Endowing vision-language models with spatial reasoning capabilities. In *Proceedings of the IEEE/CVF Conference on Computer Vision and Pattern Recognition*, pp. 14455–14465, 2024a.

Chen, J., Zhu, D., Shen, X., Li, X., Liu, Z., Zhang, P., Krishnamoorthi, R., Chandra, V., Xiong, Y., and Elhoseiny, M. Minigpt-v2: large language model as a unified interface for vision-language multi-task learning. *arXiv preprint arXiv:2310.09478*, 2023.

Chen, Z., Wang, W., Cao, Y., Liu, Y., Gao, Z., Cui, E., Zhu, J., Ye, S., Tian, H., Liu, Z., et al. Expanding performance boundaries of open-source multimodal models with model, data, and test-time scaling. *arXiv preprint arXiv:2412.05271*, 2024b.

Cheng, A.-C., Yin, H., Fu, Y., Guo, Q., Yang, R., Kautz, J., Wang, X., and Liu, S. Spatialrgpt: Grounded spatial reasoning in vision-language models. *Advances in Neural Information Processing Systems*, 37:135062–135093, 2024.

Ding, J., Xue, N., Xia, G.-S., Bai, X., Yang, W., Yang, M. Y., Belongie, S., Luo, J., Datcu, M., Pelillo, M., et al. Object detection in aerial images: A large-scale benchmark and challenges. *IEEE transactions on pattern analysis and machine intelligence*, 44(11):7778–7796, 2021.

Fiaz, M., Debary, H., Fraccaro, P., Paudel, D., Van Gool, L., Khan, F., and Khan, S. Geovlm-r1: Reinforcement fine-tuning for improved remote sensing reasoning. *arXiv preprint arXiv:2509.25026*, 2025.

Fu, X., Hu, Y., Li, B., Feng, Y., Wang, H., Lin, X., Roth, D., Smith, N. A., Ma, W.-C., and Krishna, R. Blink: Multi-modal large language models can see but not perceive. In *European Conference on Computer Vision*, pp. 148–166. Springer, 2024.

Guo, D., Yang, D., Zhang, H., Song, J., Zhang, R., Xu, R., Zhu, Q., Ma, S., Wang, P., Bi, X., et al. Deepseek-r1: Incentivizing reasoning capability in llms via reinforcement learning. *arXiv preprint arXiv:2501.12948*, 2025.

Hanyu, T., Yamazaki, K., Tran, M., McCann, R. A., Liao, H., Rainwater, C., Adkins, M., Cothren, J., and Le, N. Aerialformer: Multi-resolution transformer for aerial image segmentation. *Remote Sensing*, 16(16):2930, 2024.

Hu, Y., Yuan, J., Wen, C., Lu, X., Liu, Y., and Li, X. Rsgpt: A remote sensing vision language model and benchmark. *ISPRS Journal of Photogrammetry and Remote Sensing*, 224:272–286, 2025.

Huang, S., He, S., Qin, H., and Wen, B. Score: Scene context matters in open-vocabulary remote sensing instance segmentation. *arXiv preprint arXiv:2507.12857*, 2025a.

Huang, S., He, S., and Wen, B. Zori: Towards discriminative zero-shot remote sensing instance segmentation. In *Proceedings of the AAAI Conference on Artificial Intelligence*, volume 39, pp. 3724–3732, 2025b.

Huang, W., Jia, B., Zhai, Z., Cao, S., Ye, Z., Zhao, F., Xu, Z., Hu, Y., and Lin, S. Vision-r1: Incentivizing reasoning capability in multimodal large language models. *arXiv preprint arXiv:2503.06749*, 2025c.

Jiang, C., Zhou, Y., Yan, J., and Li, J. Grasp: Geospatial pixel reasoning via structured policy learning. *arXiv preprint arXiv:2508.17102*, 2025.

Koksal, A. and Alatan, A. A. Tinyrs-r1: Compact multimodal language model for remote sensing. *arXiv preprint arXiv:2505.12099*, 2025.

Kuckreja, K., Danish, M. S., Naseer, M., Das, A., Khan, S., and Khan, F. S. Geochat: Grounded large vision-language model for remote sensing. In *Proceedings of the IEEE/CVF Conference on Computer Vision and Pattern Recognition*, pp. 27831–27840, 2024.

Li, K., Xin, Z., Pang, L., Pang, C., Deng, Y., Yao, J., Xia, G., Meng, D., Wang, Z., and Cao, X. Segearth-r1: Geospatial pixel reasoning via large language model. *arXiv preprint arXiv:2504.09644*, 2025a.

Li, X., Ding, J., and Elhoseiny, M. Vrsbench: A versatile vision-language benchmark dataset for remote sensing image understanding. *Advances in Neural Information Processing Systems*, 37:3229–3242, 2024.

Li, Z., Muhtar, D., Gu, F., He, Y., Zhang, X., Xiao, P., He, G., and Zhu, X. Lhrs-bot-nova: Improved multimodal large language model for remote sensing vision-language interpretation. *ISPRS Journal of Photogrammetry and Remote Sensing*, 227:539–550, 2025b.

Liu, F., Emerson, G., and Collier, N. Visual spatial reasoning. *Transactions of the Association for Computational Linguistics*, 11:635–651, 2023.

Liu, F., Chen, D., Guan, Z., Zhou, X., Zhu, J., Ye, Q., Fu, L., and Zhou, J. Remoteclip: A vision language foundation model for remote sensing. *IEEE Transactions on Geoscience and Remote Sensing*, 62:1–16, 2024a.

Liu, H., Li, C., Li, Y., and Lee, Y. J. Improved baselines with visual instruction tuning. In *Proceedings of the IEEE/CVF conference on computer vision and pattern recognition*, pp. 26296–26306, 2024b.

Liu, J., Sun, L., Fu, R., and Yang, B. Towards faithful reasoning in remote sensing: A perceptually-grounded geospatial chain-of-thought for vision-language models. *arXiv preprint arXiv:2509.22221*, 2025.

Liu, S., Ma, Y., Zhang, X., Wang, H., Ji, J., Sun, X., and Ji, R. Rotated multi-scale interaction network for referring remote sensing image segmentation. In *Proceedings of the IEEE/CVF Conference on Computer Vision and Pattern Recognition*, pp. 26658–26668, 2024c.

Liu, Y., Duan, H., Zhang, Y., Li, B., Zhang, S., Zhao, W., Yuan, Y., Wang, J., He, C., Liu, Z., et al. Mmbench: Is your multi-modal model an all-around player? In *European conference on computer vision*, pp. 216–233. Springer, 2024d.

Lobry, S., Marcos, D., Murray, J., and Tuia, D. Rsvqa: Visual question answering for remote sensing data. *IEEE Transactions on Geoscience and Remote Sensing*, 58(12): 8555–8566, 2020.

Lu, X., Wang, B., Zheng, X., and Li, X. Exploring models and data for remote sensing image caption generation. *IEEE Transactions on Geoscience and Remote Sensing*, 56(4):2183–2195, 2017.

Luo, J., Pang, Z., Zhang, Y., Wang, T., Wang, L., Dang, B., Lao, J., Wang, J., Chen, J., Tan, Y., and Li, Y. Skysensegpt: A fine-grained instruction tuning dataset and model for remote sensing vision-language understanding. *arXiv preprint arXiv:2406.10100*, 2024.

Ma, Y. J., Hejna, J., Fu, C., Shah, D., Liang, J., Xu, Z., Kirmani, S., Xu, P., Driess, D., Xiao, T., et al. Vision language models are in-context value learners. In *The Thirteenth International Conference on Learning Representations*, 2024.

Majumdar, A., Ajay, A., Zhang, X., Putta, P., Yenamandra, S., Henaff, M., Silwal, S., Mcvay, P., Maksymets, O., Arnaud, S., et al. Openeqa: Embodied question answering in the era of foundation models. In *Proceedings of the IEEE/CVF conference on computer vision and pattern recognition*, pp. 16488–16498, 2024.

Muhtar, D., Li, Z., Gu, F., Zhang, X., and Xiao, P. Lhrs-bot: Empowering remote sensing with vgi-enhanced large multimodal language model. In *European Conference on Computer Vision*, pp. 440–457. Springer, 2024.

Muhtar, D., Zhang, E., Li, Z., Gu, F., He, Y., Xiao, P., and Zhang, X. Quality-driven curation of remote sensing vision-language data via learned scoring models. *arXiv preprint arXiv:2503.00743*, 2025.

Ning, H., Zhao, B., and Yuan, Y. Semantics-consistent representation learning for remote sensing image–voice retrieval. *IEEE Transactions on Geoscience and Remote Sensing*, 60:1–14, 2021.

Ou, R., Hu, Y., Zhang, F., Chen, J., and Liu, Y. Geopix: A multimodal large language model for pixel-level image understanding in remote sensing. *IEEE Geoscience and Remote Sensing Magazine*, 2025.

Pang, C., Weng, X., Wu, J., Li, J., Liu, Y., Sun, J., Li, W., Wang, S., Feng, L., Xia, G.-S., et al. Vhm: Versatile and honest vision language model for remote sensing image analysis. In *Proceedings of the AAAI Conference on Artificial Intelligence*, volume 39, pp. 6381–6388, 2025.

Radford, A., Kim, J. W., Hallacy, C., Ramesh, A., Goh, G., Agarwal, S., Sastry, G., Askell, A., Mishkin, P., Clark, J., et al. Learning transferable visual models from natural language supervision. In *International conference on machine learning*, pp. 8748–8763. PMLR, 2021.

Rafailov, R., Sharma, A., Mitchell, E., Manning, C. D., Ermon, S., and Finn, C. Direct preference optimization: Your language model is secretly a reward model. *Advances in neural information processing systems*, 36: 53728–53741, 2023.

Schulman, J., Wolski, F., Dhariwal, P., Radford, A., and Klimov, O. Proximal policy optimization algorithms. *arXiv preprint arXiv:1707.06347*, 2017.

Shabbir, A., Zumri, M., Bennamoun, M., Khan, F. S., and Khan, S. Geopixel: Pixel grounding large multimodal model in remote sensing. *arXiv preprint arXiv:2501.13925*, 2025.

Shao, Z., Wang, P., Zhu, Q., Xu, R., Song, J., Bi, X., Zhang, H., Zhang, M., Li, Y., Wu, Y., et al. Deepseekmath: Pushing the limits of mathematical reasoning in open language models. *arXiv preprint arXiv:2402.03300*, 2024.

Shen, H., Liu, P., Li, J., Fang, C., Ma, Y., Liao, J., Shen, Q., Zhang, Z., Zhao, K., Zhang, Q., et al. Vlm-r1: A stable and generalizable r1-style large vision-language model. *arXiv preprint arXiv:2504.07615*, 2025.

Sun, Y., Feng, S., Li, X., Ye, Y., Kang, J., and Huang, X. Visual grounding in remote sensing images. In *Proceedings of the 30th ACM International conference on Multimedia*, pp. 404–412, 2022.

Tian, K., Mao, J., Zhang, Y., Jiang, J., Zhou, Y., and Tu, Z. Nuscenes-spatialqa: A spatial understanding and reasoning benchmark for vision-language models in autonomous driving. *arXiv preprint arXiv:2504.03164*, 2025.

Wang, D., Zhang, J., Du, B., Xu, M., Liu, L., Tao, D., and Zhang, L. Samrs: Scaling-up remote sensing segmentation dataset with segment anything model. *Advances in Neural Information Processing Systems*, 36:8815–8827, 2023.

Wang, J., Ming, Y., Shi, Z., Vineet, V., Wang, X., Li, S., and Joshi, N. Is a picture worth a thousand words? delving into spatial reasoning for vision language models. *Advances in Neural Information Processing Systems*, 37: 75392–75421, 2024a.

Wang, Z., Prabha, R., Huang, T., Wu, J., and Rajagopal, R. Skyscript: A large and semantically diverse vision-language dataset for remote sensing. In *Proceedings of the AAAI Conference on Artificial Intelligence*, volume 38, pp. 5805–5813, 2024b.

Xie, Y., Li, G., Xu, X., and Kan, M.-Y. V-dpo: Mitigating hallucination in large vision language models via vision-guided direct preference optimization. *arXiv preprint arXiv:2411.02712*, 2024.

Yang, Y., He, X., Pan, H., Jiang, X., Deng, Y., Yang, X., Lu, H., Yin, D., Rao, F., Zhu, M., et al. R1-onevision: Advancing generalized multimodal reasoning through cross-modal formalization. *arXiv preprint arXiv:2503.10615*, 2025.

Yao, L., Liu, F., Lu, H., Zhang, C., Min, R., Xu, S., Di, S., and Peng, P. Remotereasoner: Towards unifying geospatial reasoning workflow. *arXiv preprint arXiv:2507.19280*, 2025.

Yao, X., Han, J., Cheng, G., Qian, X., and Guo, L. Semantic annotation of high-resolution satellite images via weakly supervised learning. *IEEE Transactions on Geoscience and Remote Sensing*, 54(6):3660–3671, 2016.

Yu, L., Poirson, P., Yang, S., Berg, A. C., and Berg, T. L. Modeling context in referring expressions. In *European conference on computer vision*, pp. 69–85. Springer, 2016.

Yuan, Z., Mou, L., Hua, Y., and Zhu, X. X. Rrsis: Referring remote sensing image segmentation. *arXiv preprint arXiv:2306.08625*, 2023.

Zhai, S., Bai, H., Lin, Z., Pan, J., Tong, P., Zhou, Y., Suhr, A., Xie, S., LeCun, Y., Ma, Y., et al. Fine-tuning large vision-language models as decision-making agents via reinforcement learning. *Advances in neural information processing systems*, 37:110935–110971, 2024.

Zhan, Y., Xiong, Z., and Yuan, Y. Rsvg: Exploring data and models for visual grounding on remote sensing data. *IEEE Transactions on Geoscience and Remote Sensing*, 61:1–13, 2023.

Zhang, J., Cai, M., Xie, T., and Lee, Y. J. Countercurate: Enhancing physical and semantic visio-linguistic compositional reasoning via counterfactual examples. *arXiv preprint arXiv:2402.13254*, 2024a.

Zhang, Z., Zhao, T., Guo, Y., and Yin, J. Rs5m and georsclip: A large scale vision-language dataset and a large vision-language model for remote sensing. *IEEE Transactions on Geoscience and Remote Sensing*, 2024b.

Zhang, Z., Guan, Z., Zhao, T., Shen, H., Li, T., Cai, Y., Su, Z., Liu, Z., Yin, J., and Li, X. Geo-r1: Improving few-shot geospatial referring expression understanding with reinforcement fine-tuning. *arXiv preprint arXiv:2509.21976*, 2025.